THE JOURNAL OF BIOLOGICAL CHEMISTRY
Vol. 277, No. 29, Issue of July 19, pp. 26508–26516, 2002

Printed in U.S.A.

Kinetic and Binding Analysis of the Catalytic Involvement of Ribose Moieties of a *trans*-Acting δ Ribozyme*

Received for publication, April 10, 2002, and in revised form, May 14, 2002
Published, JBC Papers in Press, May 15, 2002, DOI 10.1074/jbc.M203468200

Karine Fiola‡ and Jean-Pierre Perreault§

From the RNA Group/Groupe ARN, Département de Biochimie, Université de Sherbrooke, Sherbrooke, Québec J1H 5N4, Canada

We have identified ribose 2′-hydroxyl groups (2′-OHs) that are critical for the activity of a *trans*-cleaving δ ribozyme derived from the antigenomic strand of the hepatitis δ virus. Initially, an RNA-DNA mixed ribozyme composed of 26 deoxyribo- (specifically the nucleotides forming the P2 stem and the P4 stem-loop) and 31 ribonucleotides (those forming the catalytic center) was engineered. This mixed ribozyme catalyzed the cleavage of a small substrate with kinetic parameters virtually identical to those of the all-RNA ribozyme. The further substitution of deoxyribose for ribose residues permitted us to investigate the contribution of all 2′-OHs to catalysis. Determination of the kinetic parameters for the cleavage reaction of the resulting ribozymes revealed (i) 10 2′-OH groups appear to be important in supporting the formation of several hydrogen bonds within the catalytic core, (ii) none of the important 2′-OHs seem to coordinate a magnesium cation, and (iii) 1 of the tested RNA-DNA mixed polymers appeared to stabilize the ribozyme-substrate transition-state complex, resulting in an improvement over the all-RNA counterpart. The contribution of the 2′-OHs to the catalytic mechanism is discussed, and differences with the crystal structure of a genomic δ self-cleaved product are explained. Clearly, the 2′-OHs are essential components of the network of interactions involved in the formation of the catalytic center of the δ ribozyme.

Both genomic and antigenomic hepatitis δ virus RNAs exhibit self-cleavage activity, a process involved in viral replication (for reviews, see Ref. 1 and 2). Like other small catalytically active ribozymes, δ ribozymes cleave a phosphodiester bond of their RNA substrates, yielding reaction products containing a 5′-hydroxyl and a 2′,3′-cyclic phosphate termini. *Trans*-acting ribozymes (Rz)[1] have been developed by removing the J1/2 junction, producing one molecule possessing the substrate (S) sequence and the other possessing the catalytic domain (Rz) (Fig. 1). According to the pseudoknot model, which is well supported by experimental data, the secondary structure of δ ribozymes consists of one stem (P1), one pseudoknot (P2), two stem-loops (P3-L3 and P4-L4), and three single-stranded junctions referred to as the linker stems (J1/2, J1/4, and J4/2) (Fig. 1; see Refs. 1 and 2). It has been reported that after the formation of the P1 stem, an additional pseudoknot, named P1.1, consisting of two base pairs (bp) composed of nucleotides of the J1/4 junction and the P3 loop, was also formed (1, 3, 4).

It has been demonstrated that imidazole buffer rescues the activity of a mutant antigenomic-derived δ ribozyme possessing U76 instead of the usual C76 (referred as C47 in the *trans*-acting δ ribozyme used here) (5). This result suggests that C76 acts as a general base in the catalytic mechanism. However, it has been shown that the corresponding cytosine residue (C75) of a genomic-derived ribozyme acts as a general acid in the presence of a bound hydrated metal hydroxide acting as a base (6). In the latter report, it was also shown that in the absence of bivalent cation, a very high concentration of NaCl supports the cleavage activity although at a pH near 5.0. The ability of δ ribozyme to efficiently carry out general acid-base catalysis appears to be unique among all known catalytic RNAs (6).

δ ribozyme has a highly ordered catalytic center that is revealed by a number of unusual properties reported for *cis*-acting versions as compared with other self-cleaving RNA motifs (2). For example, it is extremely stable, with an optimal reaction temperature of about 65 °C, and retains activity at temperatures as high as 80 °C and in buffer containing 5 M urea or 18 M formamide. Based on the crystal structure of a self-cleaved genomic δ RNA, several tertiary interactions were proposed to take place within the catalytic core of the ribozyme (3, 7). The 2′-hydroxyl groups (2′-OHs) of ribonucleotides appear to be key players in a number of these interactions. More generally, 2′-OHs were shown to contribute to the catalytic mechanism of various RNA molecules, to ensure an efficient catalytic core structure, and to bind to other macromolecules or cofactors including bivalent cations (8–15). However, in the case of δ ribozyme, the identification in solution of the 2′-OH(s) important for its catalysis remains to be performed. This information is of primary importance to be able to better understand the molecular mechanism of this catalytic RNA.

The chemical synthesis of RNA polymers permits the use of site-specific functional modifications (*e.g.* the substitution of deoxyriboses (2′-H) for riboses (2′-OH)) to identify the chemical groups that make important contributions to the activity of an RNA species (for a review, see Ref. 8). The main limiting factor in this approach is the size of the RNA molecule. The 57-nucleotide (nt) δ ribozyme derived from the antigenomic RNA strand of the hepatitis δ virus (Refs. 16 and 17; Fig. 1) is too large for efficient chemical synthesis. Consequently, we tried to both remove and shorten the structural P4 stem because this approach had been shown to work for a genomic δ ribozyme (18). All mutants tested did not work, indicating that this was

* This work was supported by a grant from the Canadian Institutes of Health Research (CIHR) (to J. P. P.). The costs of publication of this article were defrayed in part by the payment of page charges. This article must therefore be hereby marked "*advertisement*" in accordance with 18 U.S.C. Section 1734 solely to indicate this fact.

‡ Recipient of a pre-doctoral fellowship from the Fonds pour la formation de Chercheurs et Aide à la Recherche (FCAR) and Fonds de la Recherche en Santé du Québec (FRSQ).

§ Canadian Institutes of Health Research scholar. To whom correspondence should be addressed. Tel.: 819-564-5310; Fax: 819-564-5340; E-mail: jperre01@courrier.usherb.ca.

[1] The abbreviations used are: Rz, ribozyme; 2′-H, 2′-hydrogen atom; 2′-OH, 2′-hydroxyl group; nt, nucleotide(s); δRD-Rz, δRNA-DNA ribozyme; S, substrate.

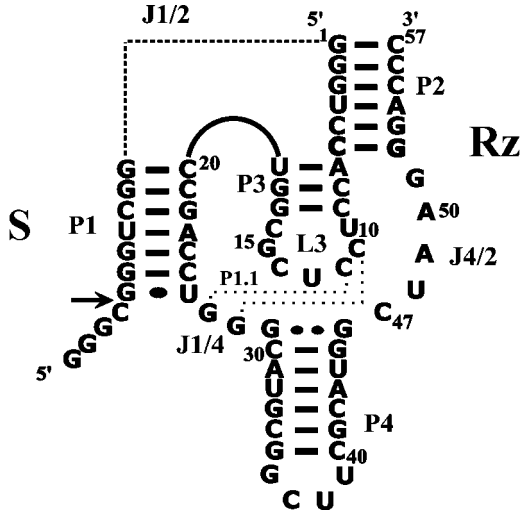

FIG. 1. **Secondary structure of the engineered antigenomic *trans*-acting δ ribozyme.** This *trans*-acting δ ribozyme system was reported previously (*e.g.* see Refs. 16 and 17). The *dashed line* represents a single-stranded region joining the substrate (*S*) and the ribozyme (*Rz*) molecules present in the *cis* form (namely J1/2) that was eliminated to produce this *trans*-acting ribozyme. The pseudoknot P1.1 is illustrated by *dotted lines*. The homopurine base pair at the top of the P4 stem is represented by *two large dots* (G●●G), whereas the wobble base pair is represented by a *single large dot* (G●U). The *arrow* indicates the cleavage site.

not a viable approach.[2] Consequently, we designed a two-piece ribozyme (19). This two-piece version required a higher concentration of magnesium (22 mM as compared with 2–3 mM for the 1 piece) to obtain the same half-maximal velocity (16) (this has been observed with other two-pieces δ ribozymes; see Ref. 20 and 21). These versions of the ribozyme may fold differently than their one-piece counterpart and are, therefore, not appropriate for this study. In this work, we use an RNA-DNA mixed ribozyme with P2 and P4 stems, which surround the catalytic center, composed exclusively of deoxyribonucleotides except for one base pair in each stem. Because this RNA-DNA mixed ribozyme has kinetic parameters virtually identical to those of the all-RNA version, we used this new tool to identify all 2′-OHs important in supporting the cleavage activity of the *trans*-acting δ ribozyme.

EXPERIMENTAL PROCEDURES

Chemical RNA Synthesis

The chemical synthesis of ribozymes, substrates, and analogue was performed using 2′-ACE chemistry (Dharmacon Research Inc., Lafayette, Colorado). The resulting polymers were deprotected according to the manufacturer's recommended protocol and purified by denaturing in 10 or 20% PAGE (19:1 ratio of acrylamide to bisacrylamide) using 45 mM Tris borate, pH 7.5, 7 M urea, and 1 mM EDTA solution as buffer. The products were visualized by UV-shadowing, and the bands corresponding to the correct sizes were cut out. The nucleic acid were then eluted from these gel slices by incubating overnight at room temperature in a solution containing 0.1% SDS and 0.5 M ammonium acetate. The RNA and RNA-DNA mixed polymers were then precipitated by the addition of 0.1 volume of 3 M sodium acetate, pH 5.2, and 2.2 volumes of ethanol, and their quantity was determined by spectrophotometry at 260 nm after dissolving in water.

End-labeling of Polymers with [γ-^{32}P] ATP

Purified RNA and RNA-DNA mixed polymers (5 pmol) were 5′-end-labeled in a final volume of 10 μl containing 3.2 pmol of [γ-^{32}P]ATP (6000 Ci/mmol; PerkinElmer Life Sciences) and 6 units of T4 polynucleotide kinase, as recommended by the enzyme manufacturer (Amersham Biosciences), at 37 °C for 45 min and then purified on 10 or 20% PAGE gels and recovered as described above.

[2] L. Bergeron and J. P. Perreault, unpublished data.

Nuclease Digestion and Alkaline Hydrolysis

The length and position of the deoxyribonucleotides in the RNA-DNA polymers were verified by alkaline hydrolysis and ribonuclease T_1 digestion (RNase T_1, which digests Gp↓N linkages in single-stranded RNA) digestion. In the enzymatic digestion, trace amounts of the 5′-end-labeled polymers (<1 nM, ~ 50 000 cpm) were dissolved in 4 μl of buffer containing 50 mM Tris-HCl, pH 7.5, 10 mM $MgCl_2$, and 100 mM NH_4Cl. The mixtures were incubated for 0.5 min at 37 °C in the presence of 5 units of RNase T_1 (Amersham Biosciences) and then quenched by adding 5 μl of loading buffer (97% formamide, 1 mM EDTA, 0.05% xylene cyanol). For alkaline hydrolysis, the 5′-end-labeled polymers (~50,000 cpm) were resuspended in 4 μl of water and 1 μl of 2 N NaOH was added. The reaction was incubated at room temperature for 5 min and then quenched by the addition of 8 μl of 500 mM Tris-HCl, pH 7.5, and 5 μl of loading buffer. The resulting mixtures were separated on denaturating 10% PAGE gels and visualized by exposure of the gels to phosphorimaging screens.

Cleavage Reactions

Various concentrations of ribozymes mixed with trace amounts of 5′-end-labeled substrate (< 1 nM) were resuspended in 32 μl of ultrapure water, heated at 90 °C for 2 min, and snap-cooled on ice for 2 min. The volume was then made up to 36 μl by adding 500 mM Tris-HCl, pH 7.5, to a final concentration of 50 mM. The mixtures were then preincubated at 37 °C for 5 min before the addition of $MgCl_2$ to 10 mM (final concentration), thereby initiating the reaction. The reactions were incubated at 37 °C and followed for either 2 or 24 h. Aliquots (4 μl) were periodically removed and quenched by the addition of 8 μl of stop solution (97% formamide, 10 mM EDTA, 0.05% bromphenol blue, and 0.05% xylene cyanol). The resulting samples were fractionated by denaturing 20% PAGE. Both the 11-nt substrate and 4-nt product bands were detected using a Molecular Dynamic PhosphorImager after exposure of the gels to phosphorimaging screens. The screens were scanned and analyzed to determine percentage of cleavage using ImageQuant, version 5.0 (Molecular Dynamics).

Kinetic Analysis

Measurement of Pseudo First-order Rate Constant (k_2, K_m', k_2/K_m', and K_{Mg})—Kinetic analyses were performed under single turnover conditions as described previously (16, 22). Briefly, trace amounts of 5′-end-labeled substrate (< 1 nM) were cleaved by various ribozyme concentrations (5–300 nM). The fractions cleaved were determined, and the rate of cleavage (k_{obs}) was obtained by fitting the data to the equation $A_t = A_\infty (1 - e^{-kt})$, where A_t is the percentage of cleavage at time t, A_∞ is the maximum percent cleavage (or the end point of cleavage), and k is the rate constant (k_{obs}). Each rate constant was calculated from at least two independent measurements. The values of k_{obs} obtained were then plotted as a function of ribozyme concentration to determine the other kinetic constants (k_2, K_m', and k_2/K_m'). The magnesium dependence for each Rz was studied by incubating the reaction mixtures with various $MgCl_2$ concentrations (1–100 mM) in the presence of an excess of ribozyme (100 nM) over substrate (< 1 nM). The concentrations of magnesium at the half-maximal velocity (K_{Mg}) were determined.

Determination of the Equilibrium Dissociation Constants (K_d)—To evaluate the formation of the RzS complex, the equilibrium constants (K_d) were determined by electrophoresis mobility shift assay by mixing ribozyme concentrations ranging from 0 to 50 nM with trace amounts of 5′-end-labeled analogue (<1 nM) in 9 μl of ultrapure water. The mixtures were then heated at 95 °C for 2 min and cooled to 37 °C for 5 min before the addition of buffer (to a final concentration of 50 mM Tris-HCl, pH 7.5, and 10 mM $MgCl_2$) in a manner analogous to that of the cleavage reaction. The samples were incubated for 1 h at 37 °C, then 2 μl of loading solution (50% glycerol, 0.025% of each bromphenol blue and xylene cyanol) were added, and the resulting mixtures were separated through native 15% PAGE gels (29:1 ratio acrylamide to bisacrylamide) in a buffer containing 45 mM Tris borate, pH 7.5, and 10 mM $MgCl_2$. The migrations were performed at 150 V for 5 h at 4 °C. The gels were exposed to phosphorimaging screens that were then scanned and analyzed using ImageQuant software to determine the amounts of bound and free analogue. Each equilibrium constant was calculated from at least two independent experiments.

RESULTS

Development of δRNA-DNA Ribozyme (δRD-Rz)

Because the studied version of δ ribozyme can be neither significantly reduced in size nor separated into two smaller

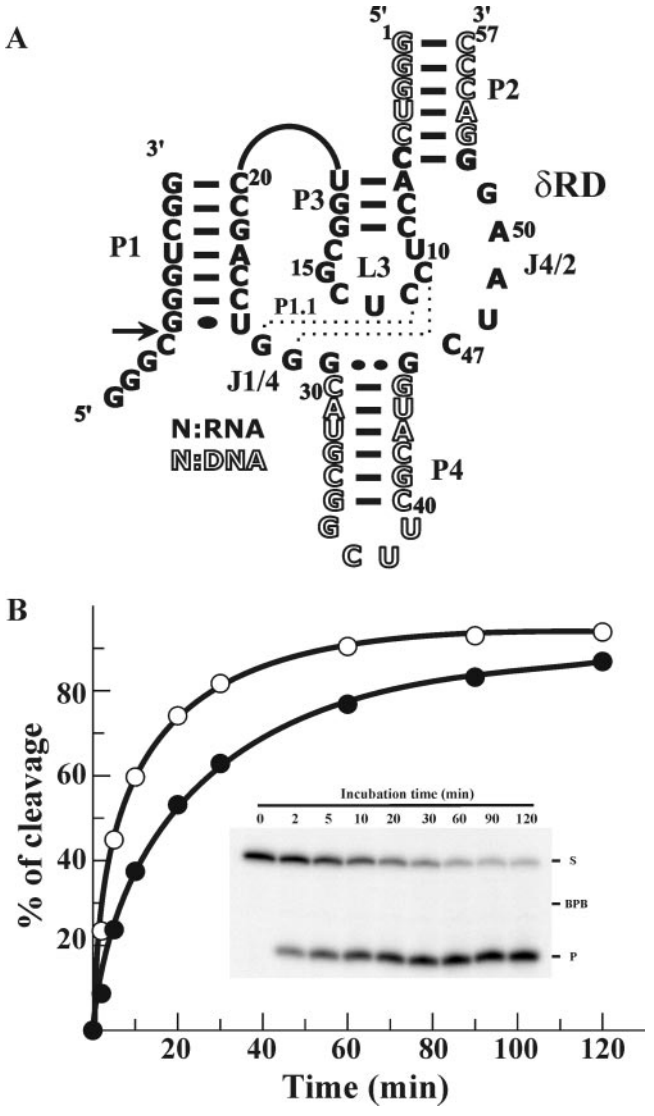

FIG. 2. **Structure and cleavage activity of δ RD-Rz as compared with δR-Rz.** *Panel A*, sequence and secondary structure of δRD-Rz. The nomenclature is according to δR-Rz (Fig. 1), except that the *outline letters* represent deoxyribonucleotides. *Panel B*, graphical representation of time courses for the cleavage reactions, catalyzed by δ R-Rz (*opened circles*) and δRD-Rz (*closed circles*). The *insets* show a typical autoradiogram of the denaturing PAGE gel for the analysis of the cleavage reaction with δRD-Rz. The positions of the bromphenol blue (*BPB*), the 11-nt substrate (*S*), and the 4-nt product (*P*) are indicated.

RNA strands, the first step of this project was the development of a version of δ ribozyme containing fewer ribonucleotides. The catalytic core of δ ribozyme is surrounded by both the P2 stem and the P4-L4 stem-loop, which were proposed to play solely structural roles (1). Consequently, we postulated that an RNA-DNA version including a P2 stem and a P4-L4 stem-loop composed of deoxyribonucleotides should be active (Fig. 2*A*). One base pair in each stem was made of ribonucleotides so as to favor their folding into a typical RNA A-helix rather than into a DNA B-helix (12). To simplify, the RNA-DNA mixed version, which includes 26 deoxyribo- and 31 ribonucleotides, will be referred as the δRNA-DNA-ribozyme (δRD-Rz), whereas the all-ribonucleotide version is referred to as the δRNA-ribozyme (δR-Rz).

The presence of deoxyribonucleotides in both the P2 stem and the P4-L4 stem-loop was confirmed by alkaline hydrolysis and RNase T_1 digestion (see "Experimental Procedures," data not shown). The ability of both δR- and δRD-Rz to cleave a model substrate, giving rise to products of 4 and 7 nt, was then tested under single turnover conditions. Trace amounts of 5′-end-labeled substrate (<1 nM) were incubated in the presence of an excess of either δR- or δRD-Rz (100 nM), and aliquots were removed at various times (Fig. 2*B*). The two ribozymes had almost identical maximal cleavage percentages (end point) of 89 and 85%, respectively. However, the cleavage rate (k_{obs}) of δRD-Rz was 2-fold slower than that of δR-Rz (*i.e.* 0.05 min^{-1} compared with 0.11 min^{-1}). We performed extensive kinetic analyses to accurately compare the cleavage abilities of δR- and δRD-Rz. Pseudo first-order cleavage rate constants (k_2 and K_m') were measured in the presence of an excess of ribozyme (5–300 nM) and trace amounts of 5′-end-labeled substrate (<0.1 nM) (Table I). Both the k_2 and K_m' values of δRD-Rz were 3-fold lower than those of δR-Rz, producing similar apparent second-order rate constants ($k_2/K_m' = 2.1 \times 10^7$ $min^{-1}M^{-1}$).

The difference in the binding between the substrate and either δRD-Rz or δR-Rz was studied by electrophoresis mobility shift assay performed under conditions similar to those used in the cleavage assays. Trace amounts of 5′-end-labeled SdC4 analogue were incubated at 37 °C with various concentrations of ribozyme, and the mixtures were then analyzed on native polyacrylamide gels. The SdC4 analogue is an 11-nt RNA identical to the substrate except for the presence of a deoxyribose residue at position 4 (*i.e.* the cleavage site), and therefore, is not cleavable. It has been shown in inhibition experiments that the use of the SdC4-analogue mimics the formation of the P1 stem in the ribozyme-substrate complex (16). The dissociation constant (K_d) decreased 3-fold for δRD-Rz as compared with δR-Rz (1 and 3 nM, respectively; Table I), indicating that some minor differences exist between these two ribozymes. In contrast, both ribozymes had equal values for the Mg^{2+} concentration at the half-maximal velocity (K_{Mg} = 3.3 and 3.2 mM), showing that the magnesium dependence was similar. Although some differences do exist between them, δR- and δRD-Rz can be considered to catalyze the cleavage of a small substrate with the same efficiency.

Before substituting any more deoxyribonucleotides for the remaining ribonucleotides in δRD-Rz, we compared the effect of the substitution for a single ribose in both versions of the ribozyme. Specifically, the ribocytidine at position 47 was replaced by a deoxyribocytidine in both ribozymes. Regardless of the precise cleavage mechanism, this cytidine is crucial in the chemical step of the δ ribozyme catalysis (5, 6). Both δR-dC47 and δRD-dC47 exhibited lower cleavage activities than did the versions containing a ribocytidine at position 47. Briefly, the measured kinetic parameters showed that the inclusion of a deoxyribose at position 47 has the same effect on both ribozymes when compared with their respective non-substituted versions (Table I, compare δR-dC47 to δR and δRD-dC47 to δRD). For example, the k_2 values were at least 6-fold less for both dC47 ribozymes, whereas the K_m' values showed a 2-fold increase in both cases. Consequently, a significant decrease of 20 (δR-dC47)- and 10 (δRD-dC47)-fold in the k_2/K_m' values were observed, indicating that the 2′-OH of the C47 is critical. More importantly, these results show that the δRD-Rz might be considered as an interesting starting version for further site-specific functional modifications geared toward the elucidation of the molecular mechanism of δ ribozyme.

Substitution of 2′-OHs in the Catalytic Core

A collection of δRD-Rz including various substitutions of deoxyribonucleotides for ribonucleotides was synthesized. The incorporation of deoxyribonucleotides at the appropriate positions in all of these ribozymes was confirmed by both alkaline hydrolysis and RNase T_1 digestion (data not shown). Subse-

TABLE I
Kinetic parameters of δR-Rz, the δRD-Rz, and their dC47 counterpart

Kinetic parameters	δR	δR-dC47	δRD	δRD-dC47
K_M' (nM)	9.1 ± 1.6	19.4 ± 4.0	2.8 ± 1.0	5.0 ± 2.0
k_2 (min^{-1})	0.19 ± 0.01	0.018 ± 0.001	0.060 ± 0.003	0.010 ± 0.001
k_2/K_M' (10^7 min^{-1} M^{-1})	2.1	0.1	2.1	0.2
K_{Mg} (mM)	3.3 ± 0.8	1.1 ± 0.3	3.2 ± 1.3	1.2 ± 0.1
K_d (nM)	3.0 ± 0.4	2.2 ± 0.3	1.0 ± 0.1	0.6 ± 0.1

quently, the ability of these ribozymes to cleave a small substrate was determined. The reactions were performed for either 2 or 24 h depending upon the level of activity.

The J4/2 Junction—The J4/2 junction is the single-stranded region joining the P2 and P4 stems (*i.e.* positions 47–51). The global substitution of five deoxyriboses for the five riboses led to a ribozyme that catalyzed less than 1% of cleavage even after 24 h of incubation (Fig. 3*A*, δRD-dJ4/2), suggesting that at least 1 of these 2′-OHs is important for efficient catalysis. To identify the one(s) that is critical, the five ribonucleotides were individually substituted. As revealed in Fig. 3*A*, both the δRD-dU48 and -dA49 ribozymes exhibited the same level of activity as δRD-Rz, indicating that the absence of the 2′-OH at these positions did not affect the catalytic activity. The kinetic parameters (K_m', k_2, and k_2/K_m') of these two ribozymes were almost identical to those of δRD-Rz (Table II), showing that the introduction of an unique deoxyribose in this single-stranded region did not necessarily alter the cleavage activity. In contrast, both δRD-dC47 and δRD-dA50 exhibited reduced cleavage activity, suggesting that the presence of the 2′-OH at these positions is important for the catalysis (Fig. 3*A*). These two ribozymes had virtually identical K_m' values but significantly reduced k_2 values (*i.e.* 6- and 12-fold, respectively) as compared with δRD-Rz (Table II). Finally, the presence of a 2′-H at position 51 (δRD-dG51) led to a minor increase in k_2, whereas K_m' remained similar to that of δRD-Rz (Table II). Inclusion of a deoxyribonucleotide at the equivalent position in the bimolecular system also resulted in an improved cleavage activity (19). Most likely, δRD-dG51 adopts a conformation that slightly enhances the folding pathway that occurs before the chemical step.

The C6-G52 Base Pair—To preserve the A-helix conformation of the all-DNA P2 stem within δRD-Rz, the C6-G52 base pair at the bottom of this stem was kept as RNA (Fig. 2*A*). The importance of the 2′-OHs at these two positions was evaluated by designing the δRD-dC6dG52 ribozyme. This ribozyme exhibited a cleavage activity similar to that of δRD-Rz (Fig. 3*A*). Both the k_2 and K_m' values decreased 2-fold, yielding similar values for k_2/K_m' (Table II) and demonstrating that the 2′-OH at positions 6 and 52 are not important for the catalysis. Because both the P2 and P3 stems were shown to stack together (3), we believe that the presence of an RNA P3 stem was sufficient to ensure that the P2 stem folds into an A-helix conformation.

The P3 Stem—When the P3 stem was composed of either two or three deoxyribonucleotide base pairs, no cleavage was detected, even after an extensive incubation of 24 h (*δRD-dP3* and *δRD-dC8dG18dC9dG17*; Fig. 3*B*). Subsequent minimal substitutions, such as the presence of a deoxyribose at either position 7 or 8 on one strand (*i.e.* δRD-dA7 and -dC8), gave ribozymes that exhibited a lower level of cleavage activity characterized by a reduction of 5- and 7-fold, respectively, in their k_2/K_m' value as compared with δRD-Rz (Fig. 3*B*, Table II). An initial examination of *panel B* in Fig. 3 suggests that the level of cleavage of δRD-dA7 is not significantly reduced. However, the reduction in its k_2/K_m' value is largely due to the 3-fold increase of its K_m', which was not detected during the preliminary activity experiments because they were performed with a large excess of ribozyme. A more significant alteration of the catalytic activity was observed with the δRD-dC9 ribozyme. In this case, a 20-fold decrease in the k_2/K_m' value, due to a K_m' value 3-fold higher and a k_2 value 6-fold lower as compared with δRD-Rz, was observed. On the other strand, the presence of a deoxyribose at position 17 causes a dramatic decrease in the cleavage level (δRD-dG17, Fig. 3*B*). After 24 h of incubation, the percentage of cleavage was less than 5%, and a k_{obs} of 0.0021 min^{-1}, which is 25-fold slower than δRD-Rz (*i.e.* 0.05

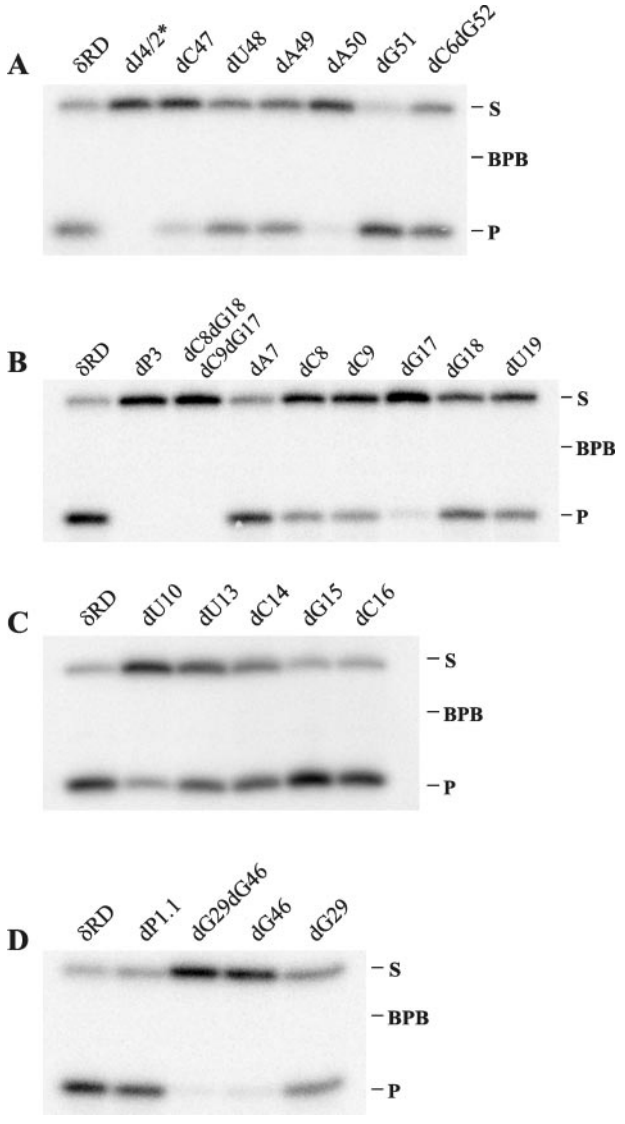

FIG. 3. **Autoradiograms of the cleavage assays with various substituted δ ribozymes.** The regions composing the δ ribozyme were studied separately. The Rz-containing deoxyribonucleotides in the J4/2 junction and P2 stem (*panel A*), the P3 stem (*panel B*), the L3 loop (*panel C*), and the P1.1 pseudoknot and the homopurine base pair (*panel D*) are shown. In each case, ribozymes (100 nM) were incubated 2 h with a trace amounts of 5′-end-labeled substrate (<1 nM), and the reaction was analyzed by denaturing 20% PAGE. The positions of bromphenol blue (*BPB*), the 11-nt substrate (*S*), and the 4-nt product (*P*) are indicated.

TABLE II
Kinetic parameters of various substituted δRD-Rz
ND, not determined.

δRD-Rz	K_M'	k_2	k_2/K_M'
	nM	min^{-1}	$10^7\ min^{-1}\ M^{-1}$
δRD	2.8 ± 1.0	0.060 ± 0.003	2.1
dJ4/2	ND	ND	ND
dC47	5.0 ± 2.0	0.010 ± 0.001	0.2
dU48	1.6 ± 0.1	0.030 ± 0.001	1.9
dA49	1.6 ± 1.0	0.023 ± 0.001	1.4
dA50	1.2 ± 0.6	0.005 ± 0.001	0.4
dG51	2.9 ± 0.5	0.17 ± 0.01	5.9
dC6-dG52	1.2 ± 0.6	0.032 ± 0.002	2.7
dP3	ND	ND	ND
dC8dG18dC9dG17	ND	ND	ND
dA7	6.8 ± 1.2	0.030 ± 0.001	0.4
dC8	2.8 ± 1.7	0.008 ± 0.001	0.3
dC9	8.2 ± 4.4	0.010 ± 0.001	0.1
dG17	ND	ND	ND
dG18	2.0 ± 0.5	0.014 ± 0.001	0.7
dU19	1.1 ± 0.6	0.011 ± 0.001	1.0
dU10	1.0 ± 0.5	0.007 ± 0.001	0.7
dU13	3.1 ± 1.4	0.017 ± 0.001	0.5
dC14	2.7 ± 1.4	0.023 ± 0.002	0.9
dG15	3.6 ± 0.9	0.074 ± 0.002	2.1
dC16	2.2 ± 0.4	0.049 ± 0.001	2.2
dP1.1	2.8 ± 1.1	0.045 ± 0.003	1.6
dG29-dG46	ND	ND	ND
dG46	ND	ND	ND
dG29	1.9 ± 1.6	0.017 ± 0.001	0.9

TABLE III
Dissociation and magnesium constants for various substituted δRD-Rz
ND, not determined.

δRD-Rz	K_d	K_{Mg}
	nM	*mM*
δRD	1.0 ± 0.1	3.2 ± 1.3
dJ4/2	0.7 ± 0.1	ND
dC47	0.6 ± 0.1	1.2 ± 0.1
dU48	0.8 ± 0.1	4.6 ± 1.2
dA49	0.9 ± 0.1	4.7 ± 2.0
dA50	0.4 ± 0.1	2.3 ± 0.8
dG51	0.8 ± 0.1	2.1 ± 0.6
dC6-dG52	0.40 ± 0.04	3.5 ± 0.4
dP3	0.5 ± 0.1	ND
dC8dG18dC9dG17	0.40 ± 0.04	ND
dA7	0.5 ± 0.1	0.9 ± 0.3
dC8	1.0 ± 0.1	0.4 ± 0.4
dC9	1.0 ± 0.1	0.6 ± 0.6
dG17	3.6 ± 0.3	ND
dG18	0.6 ± 0.1	2.1 ± 0.4
dU19	0.9 ± 0.1	1.5 ± 0.6
dU10	1.0 ± 0.1	2.0 ± 1.0
dU13	0.7 ± 0.1	2.9 ± 0.9
dC14	0.8 ± 0.1	1.7 ± 0.3
dG15	1.1 ± 0.5	5.5 ± 0.5
dC16	0.7 ± 0.1	3.4 ± 0.5
dP1.1	0.9 ± 0.2	4.5 ± 1.2
dG29-dG46	0.5 ± 0.1	ND
dG46	0.40 ± 0.04	ND
dG29	0.7 ± 0.1	1.1 ± 0.5

min^{-1}), was estimated in the presence of a ribozyme concentration of 100 nM. No other kinetic parameters could be determined because the activity was too low. Substitution of the adjacent ribose (*i.e.* δRD-dG18) also yields a lower cleavage activity than δRD-Rz although to a lower degree. In this case the k_2/K_m' value was $0.7 \times 10^7\ min^{-1}M^{-1}$, which is 3-fold less than δRD-Rz. Finally, the incorporation of a deoxyribose at position 19 (*i.e.* δRD-dU19) gave a ribozyme that exhibited almost the same level of activity as δRD-Rz (Fig. 3*B*, Table II). The slight reduction in the activity observed with this mutant was probably due to the instability caused by the presence of a RNA-DNA heteroduplex base pair and is, therefore, not indicative of an important 2′-OH group. With the exception of the 2′-OH of U19, all 2′-OHs of the P3 stem are important in the cleavage activity, albeit to different degrees.

The L3 Loop—This 7-nt loop is located in the middle of the catalytic core. Because the cytosines at positions 11 and 12 are involved in the formation of the P1.1 pseudoknot, the 2′-OHs of these residues were analyzed separately (see below). Five δRD-Rzs, each possessing one additional deoxyribose residue, were synthesized (Fig. 3*C*, Table II). The δRD-dG15 and -dC16 ribozymes exhibited the same level of cleavage and had kinetic parameters virtually identical to δRD-Rz, whereas δRD-dC14 showed a (probably) insignificant minimal decrease. Both the δRD-dU10 and -dU13 ribozymes exhibited less cleavage activity due to a significant decrease in their k_2 values as compared with that of δRD-Rz (*i.e.* 9- and 4-fold, respectively). Thus, the 2′-OH group of the residues at positions 10 and 13 in the L3 loop contribute to efficient catalysis.

The P1.1 Pseudoknot—The P1.1 pseudoknot is composed of two base pairs (*i.e.* C11G28/C12G27). The δRD-dP1.1 ribozyme, which includes deoxyribonucleotides at all four positions, exhibited the same level of cleavage and had kinetic parameters equivalent to δRD-Rz (Fig. 3*D*, Table II). Thus, the presence of only DNA base pairs in the P1.1 pseudoknot did not result in folding into a B-helix. A potential explanation for this observation is that the P1.1 pseudoknot stacks with (and between) the P1 and P4 stems, and because the P1 stem is composed of RNA and folds into an A-helix, the P1.1 pseudoknot also adopts the proper folding.

The G29-G46 Base Pair—Another particular feature of δ ribozyme is the presence of a homopurine base pair at the top of the P4 stem (*i.e.* G29-G46, Ref.1). This base pair is the only one within the P4 stem of δRD-Rz that was kept as RNA to allow the adoption of an A-helix. If deoxyribonucleotides are introduced at both positions, almost no cleavage is observed after a 24-h incubation even if the C30-G45 base pair has been synthesized as RNA to ensure proper folding (Fig. 3*D*). In the presence of 100 nM of Rz, a k_{obs} of only 0.0019 min^{-1} was estimated; consequently, no other kinetic parameters can be determined. The presence of a deoxyribonucleotide at only position 46 did not restore the cleavage activity (Fig. 3*D*, δRD-dG46; k_{obs} = 0.0022 min^{-1}). However, the level of activity was recovered with the δRD-dG29 version (Fig. 3*D*, Table II). This shows that the incorporation of one deoxyribonucleotide in the homopurine base pair is not responsible for the lower activity level. Thus, the 2′-OH of the ribose at position 46 is most likely involved in a key tertiary interaction required for efficient catalysis to occur.

K_d and K_{Mg} Determination

In general, the substituted ribozymes that exhibited different levels of activity showed variation of their k_2 values but not their K_m' values. To verify whether or not the absence of the 2′-OH affected the formation of the RzS complex, electrophoresis mobility shift assays using the SdC4 analogue were performed. The K_d values are reported in Table III. With the exception of δRD-dG17, all substituted-Rzs had K_d values varying between 0.4 and 1.1 nM; that is to say, similar to the 1.0 nM obtained for δRD-Rz. That the binding of the substrate remained unaltered suggests that the global architecture (or appropriate folding) of most of the ribozymes was not modified by the inclusion of deoxyribonucleotides. The binding of the SdC4 analogue imitates the formation of the P1 stem but not necessarily the subsequent step(s), which includes the conformational transition (16). Consequently, the significant varia-

tion of the K_m' values observed for both the δRD-dA7 and δRD-dC9 ribozymes (*i.e.* K_m' = 6.8 and 8.2 nM compared with 2.8 nM for δRD-Rz) suggests alteration of the step(s) that occurs after P1 stem formation during the folding pathway. Only the δRD-dG17 ribozyme had a K_d that was significantly altered as compared with δRD-Rz (3.6 and 1.0 nM, respectively). On its own this reduction of the binding affinity is not enough to explain the important loss of catalytic activity seen with this ribozyme (*i.e.* ~2 orders of magnitude).

In several RNA species important 2′-OHs have been shown to bind metal ions such as magnesium (10, 23). If a 2′-OH bound a Mg^{2+} ion either directly or through a solvating water molecule, the absence of this group would result in a weaker binding of the cation, yielding a lowered catalytic activity and a larger K_{Mg} value. To verify whether or not the important 2′-OHs make such a contribution to the catalytic activity, K_{Mg} values were determined for the substituted δRD-Rz (Table III). Small variations of the K_{Mg} were observed, but they did not appear to be significant when the statistical errors were taken into account, except in three cases (see below). Regardless the substituted δRD-Rz, increasing the magnesium concentration did not restore the cleavage activity (data not shown). These results lead us to conclude that no 2′-OHs in the catalytic center are involved in magnesium binding, a finding unique to the δ ribozyme. Unlike most of the substituted δRD-Rz, the δRD-dA7, -dC8, and -dC9 ribozymes had smaller K_{Mg} values (*i.e.* 0.9, 0.4, and 0.6 mM, respectively) than δRD-Rz (3.2 mM; Table III). This suggests that these ribozymes bound the Mg^{2+} ion(s) slightly more strongly, although they exhibited less activity. This difference in the magnesium dependence might result from an unusual conformation due to the presence of a deoxyribose residue within this strand of the P3 stem that favors magnesium binding to the catalytic center. Finally, because magnesium cations show cooperative binding to many RNA species, as is observed with tRNA (23), the collected data were plotted according to the Hill equation (data not shown). All ribozymes gave Hill coefficients near unity (*i.e.* 0.52–1.43 ± 0.3), leading us to conclude that the binding of magnesium to the various δ ribozymes is neither cooperative nor different, depending on the deoxyribonucleotide substitutions present.

Substitutions of the 2′-OH in the Binding Domain

The binding domain of δ ribozyme is formed by the P1 stem, which consists of 7 consecutive base pairs (6 Watson-Crick base pairs and the wobble base pair adjacent to the cleavage site; see Ref. 1). To test whether or not any of the 2′-OHs of the nucleotides within the P1 strand of the ribozyme (positions 20–26) are important, 6 substituted Rzs were synthesized. These Rzs contain only one (δRD-dG22, -dA23, -dC24, -dC25, and -dU26) or two (δRD-dC20C21) additional deoxyribonucleotides as compared with δRD-Rz. All of these ribozymes cleaved the small substrate with approximately the same efficiency as δRD-Rz (Fig. 4*A*). Regardless of the substituted-Rz, the K_m' values were virtually identical to that of δRD-Rz, whereas all had slightly smaller k_2' values (*i.e.* 2-fold), indicating that none of the 2′-OHs of the P1 strand contributes to the molecular mechanism of the catalysis (Fig. 4*B*). This conclusion received support from electrophoresis mobility shift assay experiments using the SdC4 analogue, which showed that the K_d values of these ribozymes (*i.e.* varying between 1.1 to 1.6 nM) were similar to that of δRD-Rz.

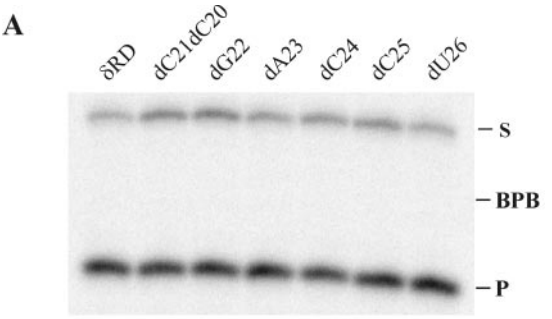

B

δRD-Rz	K_M' (nM)	k_2 (min^{-1})	k_2/K_M' (10^7min^{-1}M^{-1})
δRD	2.8 ± 1.0	0.060 ± 0.003	2.1
dC21-dC20	2.0 ± 0.2	0.023 ± 0.002	1.2
dG22	5.7 ± 1.2	0.028 ± 0.001	0.5
dA23	4.1 ± 0.8	0.033 ± 0.002	0.8
dC24	3.7 ± 1.2	0.033 ± 0.002	0.9
dC25	5.1 ± 0.9	0.032 ± 0.001	0.6
dU26	1.7 ± 0.3	0.045 ± 0.001	2.6

FIG. 4. **Analysis of the substitutions performed within the binding domain of δRD-Rz.** *Panel A*, in each case, ribozymes (100 nM) were incubated with a trace amounts of 5′-end-labeled substrate (<1 nM) for 2 h, and the mixtures were analyzed by 20% PAGE. The positions of the bromphenol blue (*BPB*), the 11-nt substrate (*S*) and the 4-nt product (*P*) are indicated. *Panel B*, kinetic parameters of the ribozyme containing substitutions within the ribozyme strand of the P1 stem.

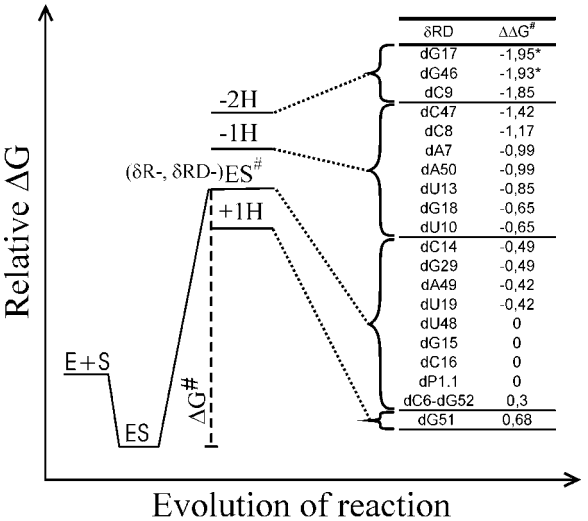

FIG. 5. **Differences in the free energy of the transition-state stabilization (ΔΔ$G^{\#}$) for the cleavage reaction catalyzed by various substituted δRD-Rz.** The representation of ΔΔ$G^{\#}$ is according to an energy profile of the proposed reaction pathway. The ΔΔ$G^{\#}$ was calculated from −RT ln [(k_2/K_m' substituted-Rz)/(k_2/K_m' δRD-Rz)], where T is 310.15 K, and R is 1.987 cal·K^{-1}·mol^{-1} (25). When available, k_2/K_m' values were used for this calculation, whereas for some ribozymes, which are denoted by a *asterisk*, k_{obs} values were used. These calculations provide ΔΔ$G^{\#}$ values that are clustered in four groups: ES$^{\#}$ (±0.5 kcal·mol^{-1})-like δRD-Rz, ES$^{\#}$ plus one H-bond (*+1H*; >0.5 kcal·mol^{-1}), ES$^{\#}$ minus one H-bond (−1H; between −0.5 and −1.5 kcal·mol^{-1}), and ES$^{\#}$ minus two H-bonds (*−2H*; >−1.5 kcal·mol^{-1}). ES, enzyme-substrate.

DISCUSSION

δRD-Rz catalyzes the cleavage of a model substrate with a constant of specificity (k_2/K_m') similar to that of its all-RNA counterpart. This suggests that the free energy of the transition-state stabilization (Δ$G^{\#}$) is similar for both δR- and δRD-Rz (Fig. 5). The large number of deoxyribonucleotides present in δRD-Rz (*i.e.* 26 of 57 nt) provides an RNA-DNA mixed ribozyme that is both more efficiently synthesized and more affordable than the all-RNA version and, therefore, constitutes an interesting tool for further progress in the elucidation of the interaction network within the catalytic core by means of site-specific functional modifications. For example, to investigate the importance of the 2′-OH of all residues present in δRD-Rz,

a collection of ribozymes including 2′-H substitutions was synthesized.

To progress in the analysis of the data, the differences in terms of the free energy of the transition-state stabilization ($\Delta\Delta G^{\#}$) between several ribozymes substituted in the catalytic center and δRD-Rz were calculated (see the legend of Fig. 5 and Ref. 25). According to the $\Delta\Delta G^{\#}$ values, the substituted ribozymes could be separated into four groups (Fig. 5) as follows. (i) The first group consists of those with k_2/K_m' values virtually identical to that of δRD-Rz and, therefore, possessing a $\Delta\Delta G^{\#}$ of or near zero ($\Delta\Delta G^{\#} \pm 0.5$ kcal/mol). In these cases the introduction of a deoxyribonucleotide(s) did not significantly affect the catalytic activity (*e.g.* δRD-dP1.1). Minimal differences may result from local structural modifications, such as a sugar pucker, that can adopt various conformations. Usually deoxyriboses favor the C2′-endo conformation, whereas riboses adopt the C3′-endo conformation due to steric hindrance in the helix structure created by the 2′-OH groups (23). (ii) The second group consists of ribozymes whose $\Delta\Delta G^{\#}$ values varied between −0.5 to −1.5 kcal/mol and are most likely those for which the RzS transition-state complex lost one hydrogen bond (H-bond). δRD-dU10 and -dG18 are at the limit of being considered as belonging to this group because they possess $\Delta\Delta G^{\#}$ values of −0.65 kcal/mol. (iii) The third group consists of three ribozymes with $\Delta\Delta G^{\#} < -1.5$ kcal/mol, which most likely represent those that have lost two H-bonds within their RzS transition-state complexes. δRD-dC47 was classified in the previous group (−1 H-bond) but had an intermediate $\Delta\Delta G^{\#}$ of −1.42 kcal/mol, so it is not impossible that it may have lost two H-bonds. (iv) Last, δRD-dG51 has a positive $\Delta\Delta G^{\#}$ of 0.68 kcal/mol, which suggests that its transition-state complex is stabilized by an additional H-bond. To our knowledge this is the first demonstration of the introduction of deoxyribose residues enhancing the activity of a catalytic RNA. In summary, 10 ribonucleotides clustered in a small region formed by the J4/2 junction, the adjacent G46 of the homopurine base pair, and the P3-L3 stem-loop harbor the critical 2′-OH groups (Fig. 6*A*). Based on the $\Delta\Delta G^{\#}$ values, these 2′-OHs are involved in the formation of 13 H-bonds. It should be noted that this number may be smaller if two 2′-OHs are used to form the same H-bond. Unfortunately, the approach used in this work does not permit the identification of the chemical groups that form an H-bond with a given 2′-OH.

In a previous study, we tested a collection of RNA/DNA-mixed substrates in which a single ribonucleotide was substituted by a deoxyribonucleotide at each position of the 11-mer (24). With the exception of the nucleotide adjacent to the cleavage site that is essential for the chemical step, no 2′-OH in the substrate contributes to the catalysis. All of these substrates were cleaved at a level ranging from 1 equivalent to that of the native substrate to one either 2-fold more or 2-fold less. It was suggested that the variability in activity resulted from differences in the binding. In summary, with the exception of the 2′-OH at position C4 on the substrate, no 2′-OH of the P1 stem is critical for the cleavage.

Important 2′-OHs have been identified from the crystal structure of a δ ribozyme (3, 7) and, therefore, could be compared with the results reported here. Unfortunately, the coordinate error of the crystal structure was 0.3–0.4 Å; consequently, all hydrogen bonds were not necessarily observed in this structure. Regardless, 9 ribose 2′-OHs were suggested to form 11 H-bonds (Fig. 6*B*). Discrepancies in the important 2′-OHs may not only be due to the fact that we compared results from a crystal study with ones performed in solution but also to other factors including the fact that the crystal structure was from (i) a *cis*-acting form of a δ ribozyme rather than a *trans*-acting version, (ii) a self-cleavage product rather than the RzS active complex, and (iii) a sequence derived from the genomic hepatitis δ virus strand rather than the antigenomic strand. These maps of important 2′-OHs show several common features as well as some differences (Fig. 6). For example, the 2′-OHs from residues C21 and the G40 were suggested to form H-bonds with the CAA sequence of the J1/4 junction (Fig. 6*B*). Because this triplet is only found in the genomic version, the equivalent 2′-OHs (positions C11 and G29) in the antigenomic ribozyme could be substituted by deoxyribonucleotides without affecting the catalytic activity (Fig. 6*A*). One of the important novelties arising from the crystal structure was the presence of a ribose zipper between the J4/2 junction and the proximal strand of the P3 stem (3, 7). Specifically, the 2′-OH of riboses A77 and A78 forms two H-bonds with the 2′-OH of C18 and C19. It appears that this structural motif contributes to the positioning of the P3 stem in the catalytic core. If the antigenomic δ ribozyme includes a ribose zipper, the participation of 2′-OH from the J4/2 junction would be limited to only one (*i.e.* the 2′-OH of A50). As a consequence, the presence of such a motif appears unlikely. However, five 2′-OHs of the six residues forming the P3 stem in the antigenomic ribozyme are suggested to form seven H-bonds (Fig. 6*A*). These 2′-OH groups may serve the same purpose of positioning the P3-L3 stem-loop within the catalytic core, thereby explaining why the ribozymes with a P3 stem formed by either 4 or 6 deoxyribonucleotides did not exhibit any detectable activity. A similar function of the positioning of helices in the active structure has been suggested for a cluster of important 2′-OHs in the *Neurospora* VS ri-

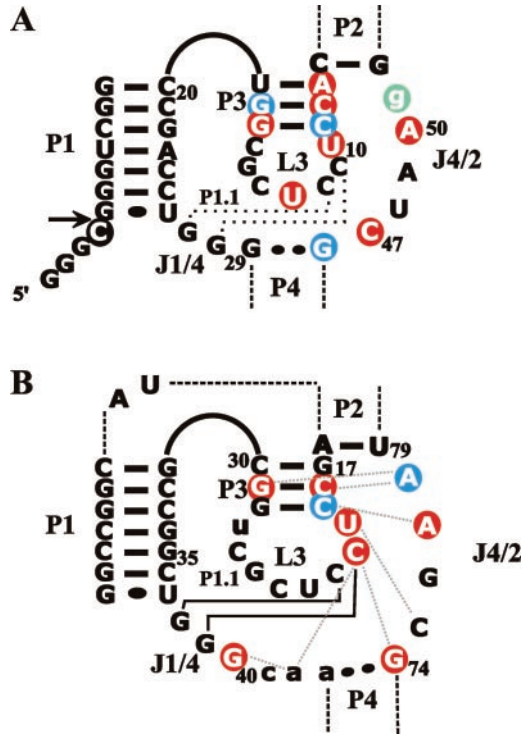

FIG. 6. **Schematic representation of the important 2′-OHs identified in the catalytic center of δ ribozymes.** *Panel A*, map of the important 2′-OHs of the antigenomic δ ribozyme according to the results presented in this paper. *Panel B*, map of the important 2′-OHs of the genomic ribozyme based on the crystal structure (3, 7). *Red* and *blue circles* indicate that the 2′-OH of the residue is suggested to form one or two H-bonds, respectively. The guanosine at position 51 (*panel A*) is *circled* in *green* to indicate that the absence of its 2′-OH allowed the formation of an additional H-bond as compared with δRD-Rz. The *black circles* show the 2′-OH adjacent to the cleavage site, which was previously reported to be essential for the chemical step (16). *Lowercase letters* mark different nucleotides between the genomic and antigenomic forms (3, 28, 32, 33). In *panel B*, *dotted lines* indicate the partner residues forming an H-bond with a 2′-OH.

bozyme (15). The formation of several H-bonds involving 2′-OH groups rather than classical base pairs in the positioning of the P3-L3 stem-loop might be considered as an innovative strategy. Although this allows for the critical positioning of the stem-loop to take place, it is probably not too stable and thereby preserves the flexibility required for the L3 loop contribution to subsequent steps in the folding pathway such as the formation of the P1.1 pseudoknot. Such a situation might help to explain the increases in K_m' observed with δRD-dA7 and -dC9 and the K_d increase with δRD-dG17 among the substituted-Rzs studied. In these cases, the absence of a 2′-OH most likely results in a slower step in the formation of the active transition-state complex, yielding a higher binding constant. These K_m' and K_d value increases were the only significant variations of these two parameters detected for all of the ribozymes tested. The effect of the absence of other important 2′-OHs was to decrease the k_2' values, suggesting a perturbation within the transition-state complex (although the exact molecular mechanism of this remains to elucidated).

In the L3 loop of the genomic ribozyme only the 2′-OH of U20 appears to be important, interacting with the base of C75 (which corresponds to U10 and C47 in the antigenomic Rz). In the antigenomic ribozyme, U10 possesses an important 2′-OH that could be involved in an equivalent interaction with C47. In addition, the 2′-OH of U13 appears to be important in the antigenomic ribozyme. However, neither the identity of the nucleotide interacting with this 2′-OH nor the H-bond in which it is involved (*i.e.* that equivalent to the one formed between C22 and the CAA triplet of the genomic ribozyme) are known. According to the crystal structure the G74 of the homopurine base pair has an important 2′-OH that contributes to one H-bond, whereas the equivalent 2′-OH in the antigenomic Rz is proposed to participate in the formation of 2 H-bonds. Finally, the C47 of the antigenomic ribozyme appears to be important, whereas the equivalent base (C75) in the genomic version does not form an H-bond (according to the crystal structure). The 2′-OH of the C47 may help in the positioning of the catalytic residue, in close proximity to the scissile phosphate. Finally, in both maps of the important 2′-OHs, none of those in the P1 stem appears to be important for the structure, whereas that at the cleavage site in the substrate is essential for the chemical step. Clearly, some 2′-OH groups are important for both the antigenomic and genomic ribozymes, whereas others are only important for one or the other, suggesting the existence of minor differences between two forms. More importantly, the 2′-OHs are key components of both catalytic centers, suggesting that they are involved in several tertiary interactions essential for the adoption of the active conformation.

It has been suggested that δ ribozyme has an absolute requirement for the presence of divalent metal ions for self-cleavage to occur under standard conditions (26). The presence of an essential metal ion coordination site(s) in this catalytic RNA is supported by several observations including (i) the displacement of lead ion(s) within a δ ribozyme by both neomycin and magnesium (27), (ii) the monitoring of three Mg^{2+} ions in a two-piece δ ribozyme by circular dichroism (18), (iii) the fact that magnesium supports structural rearrangements within a genomic δ ribozyme (based on chemical probing experiments, Ref. 29), (iv) the fact that Mg^{2+} induced a specific cleavage at position G52 at the bottom of the P2 stem, occurring solely within an antigenomic-derived, catalytically active RzS complex (24), and (v) that an NMR spectroscopic analysis of an antigenomic δ ribozyme version suggests that a catalytic Mg^{2+} ion binds to the pocket formed by P1 and L3 (30). The magnesium appears to be essential to the δ ribozyme activity, although it is unclear whether this(these) cation(s) plays an indispensable role in both the folding and active site chemistry. However, according to the crystal structure of the δ ribozyme, no tightly bound metal ion is located within the catalytic center (3, 7), suggesting that it is stabilized entirely by base-pairing, stacking, non-canonical base-backbone, and backbone-backbone interactions. Furthermore, we provide evidence that no 2′-OH contributes to the binding of Mg^{2+} ions. To explain this discrepancy, we envisaged that one, or less likely, more than one Mg^{2+} ion is located in a groove of the P3 stem either at or near the junction of the bottom of the P2 stem. This localizes the Mg^{2+} ion close enough to be responsible for the specific metal ion-induced cleavage at G52. Moreover, this may explain why the introduction of deoxyribonucleotide at positions 7–9 within one strand of the P3 stem showed small reductions in the K_{Mg} values. The resulting RNA/DNA heteroduplex base pairs are slightly less stable, probably slightly opening the stem and thereby allowing a better binding of the Mg^{2+} by a base. This Mg^{2+} ion would be stabilized in this location by interactions formed with the bases, thereby explaining why no 2′-OHs are involved. With such a localization, which is relatively far from the scissile phosphate, this Mg^{2+} ion would most likely have a role in the folding rather than in the chemical step. The lack of Mg^{2+} in the crystal structure could be explained by the fact that it was eliminated through the stabilization of some tertiary interactions, for example a ribozyme-zipper, or alternatively, a situation comparable with that found in the lead-catalyzed specific cleavage of $tRNA^{Phe}$ (31). In the uncleaved structure Pb^{2+} was observed to be bound with high frequency at the cleavage site, but once the tRNA was cleaved, the Pb^{2+} dissociated and was not observed in the cleaved structure. A similar scenario appears to be plausible as an explanation for the lack of Mg^{2+} in the cleaved form of the *cis*-acting δ ribozyme. Although this hypothesis, which remains to be supported by physical evidence, localizes only 1 Mg^{2+} ion, it does not exclude the possibility that several cations might be bound to the δ ribozyme.

In summary, this work identified all 2′-OH groups that are important for the catalytic activity of a *trans*-acting δ ribozyme. None of the 2′-OHs seem to coordinate a magnesium cation. However, they are clearly essential components of the network of interactions forming the active catalytic core of the δ ribozyme.

Acknowledgments—We acknowledge Audrey Lapierre for technical assistance in the binding shift assays. In addition, we acknowledge Drs. Jennifer Doudna and Jeremy Murray (from Yale University) as well as François Major and Nancy Bourassa (from Université de Montréal) for help in the identification of the important 2′-OH groups within the δ ribozyme crystal structure. The RNA group is supported by grants from both the Canadian Institutes of Health Research (CIHR) and Fonds pour la formation de Chercheurs et Aide à la Recherche (Québec).

REFERENCES

1. Wickham, G. S., and Been, M. D. (2002) *Cell. Mol. Life Sci.* **59,** 112–125
2. Doherty, E. A., and Doudna, J. A. (2000) *Annu. Rev. Biochem.* **69,** 597–615
3. Ferre-D'Amare, A. R., Zhou, K., and Doudna, J. A. (1998) *Nature* **395,** 567–574
4. Ananvoranich, S., and Perreault, J. P. (2000) *Biochem. Biophys. Res. Commun.* **270,** 600–607
5. Perrotta, A. T., Shih, I., and Been, M. D. (1999) *Science* **286,** 123–126
6. Nakano, S., Chadalavada, D. M., and Bevilacqua, P. C. (2000) *Science* **287,** 1493–1497
7. Ferré-D'Amaré, A. R., and Doudna, J. A. (2000) *J. Mol. Biol.* **295,** 541–556
8. Verma, S., and Eckstein, F. (1998) *Annu. Rev. Biochem.* **67,** 99–134
9. Quigley, G. J., Rich, A. (1976) *Science* **194,** 796–806
10. Jack, A., Ladner, J. E., Rhodes, D., Brown, R. S., and Klug, A. (1977) *J. Mol. Biol.* **111,** 315–328
11. Cate, J. H., Gooding, A. R., Podell, E., Zhou, K., Golden, B. L., Kundrot, C. E., Cech, T. R., and Doudna, J. A. (1996) *Science* **273,** 1678–1685
12. Egli, M., Usman, N., and Rich, A. (1993) *Biochemistry* **32,** 3221–3237
13. Perreault, J. P., Wu, T. F., Cousineau, B., Ogilvie, K. K, and Cedergren, R. (1990) *Nature* **344,** 565–567
14. Chowrira, B. M., Berzal-Herranz, A., Keller, C. F., and Burke, J. M. (1993) *J. Biol. Chem.* **268,** 19458–19462
15. Sood, V. D., Yekta, S., and Collins, R. A. (2002) *Nucleic Acids Res.* **30,** 1132–1138

16. Mercure, S., Lafontaine, D., Ananvoranich, S., and Perreault J. P. (1998) *Biochemistry* **37,** 16975–16982
17. Ananvoranich, S., and Perreault, J. P. (1998) *J. Biol. Chem.* **273,** 13182–13188
18. Fauzi, H., Chiba, A., Nishikawa, F., Kawakami, J., Roy, M., and Nishikawa, S. (1998) *Anal. Chim. Acta* **365,** 309–317
19. Ananvoranich, S., Fiola, K., Ouellet, J., Deschênes P., and Perreault, J. P. (2001) *Methods Enzymol.* **341,** 553–566
20. Sakamoto, T., Tanaka, Y., Kuwabara, T., Kim, M. H., Kurihara, Y., Katahira, M., and Uesugi, S. (1997) *J. Biochem.* **121,** 1123–1128
21. Pereira, M. J. B., Harris, D. A., Rueda, D., and Walters, N. G. (2002) *Biochemistry* **41,** 730–740
22. Hertel, K. J. Herschlag, D., and Uhlenbeck, O. C. (1996) *EMBO J.* **15,** 3751–3757
23. Saenger, W. (1984) in *Principles of Nucleic Acid Structure*, (Cantor, Charles R., ed) pp. 331–349, Springer-Verlag New York Inc., New York
24. Lafontaine, D. A., Ananvoranich, S., and Perreault, J. P (1999) *Nucleic Acids Res.* **27,** 3236–3243
25. Fersht, A. R. (1985) in *Enzyme Structure and Mechanism*, 2nd Ed., pp. 311–312, W. H. Freeman and Co., New York
26. Murray, J. B., Seyhan, A. A., Walter, N. G., Burke, J. M., and Scott, W. G. (1998) *Chem. Biol.* (*Lond.*) **5,** 587–595
27. Rogers, J., Chang, A. H., Ahsen, U. V., Schroeder, R., and Davies, J. (1996) *J. Mol. Biol.* **259,** 916–925
28. Kumar, P. K. R., Suh, Y. A., Miyashiro, H., Nishikawa, F., Kawakami, J., Taira, K., and Nishikawa, S. (1992) *Nucleic Acids Res.* **20,** 3919–3924
29. Kumar, P. K. R., Taira, K., and Nishikawa, S. (1994) *Biochemistry* **33,** 583–592
30. Tanaka, Y., Hori, T., Tagaya, M., Sakamoto, T., Kurihara, Y., Katahira, M., and Uesugi, S. (2002) *Nucleic Acids Res.* **30,** 766–774
31. Pan, T., Long, D. M., and Uhlenbeck, O. C. (1993) In *The RNA World* (Gesteland, R. F., and Atkins, J. F., eds) pp. 371–402, Cold Spring Harbor Laboratory Press, Cold Spring Harbor, NY
32. Tanner, N. K., Schaff, S., Thill, G., Petit-Koskas, E., Crain-Denoyelle, A. M., and Westhof, E. (1994) *Curr. Biol.* **4,** 488–498
33. Thill, G., Vasseur, M., and Tanner, N. K. (1993) *Biochemistry* **32,** 4254–4262